pH-Responsive Nanogels for Site-Specific Drug Delivery: Synthesis, Characterization, and Stimuli-Triggered Release Behavior

Saba Niaz [1], Sam Au [1*]

Abstract

Background: Traditional drug delivery systems face limitations such as low solubility, instability, and toxicity, which can impact efficacy and safety. pH-responsive nanogels offer an innovative approach for controlled and targeted drug delivery, particularly for oral administration, by releasing drugs based on environmental pH changes. Objective: This study aimed to synthesize and characterize novel, physically cross-linked pH-responsive nanogels using poly(L-lysine isophthalamide) grafted with decylamine (PLP-NDA) and evaluate their potential as oral drug delivery vehicles. Methods: PLP-NDA nanogels were synthesized using a surfactant-free nanoprecipitation method, combining anionic and amphiphilic properties with hydrophobic segments for stable nanogel formation and drug loading. The nanogels were characterized for particle size, zeta potential, and stability under varied ionic strengths and pH levels. Nile red (NR) was used as a model hydrophobic drug to assess encapsulation efficiency and release profiles in simulated fasted gastric (pH 1.6) and intestinal fluids (pH 6.5). Results: The synthesized PLP-NDA nanogels had an average particle size of 101.3 ± 1.2 nm and a zeta potential of -37.51 ± 3.32 mV, demonstrating stability over 28 days. Encapsulation efficiency of NR was 16.5 ± 2.1%, with a particle size of 124.5 ± 2.1 nm for PLP-NDA-NR nanogels. Drug release studies showed complete release in intestinal fluid (pH 6.5) within 24 hours, while release in gastric fluid (pH 1.6) was 54.0 ± 3.7%. Conclusion: PLP-NDA nanogels exhibit favorable characteristics for pH-triggered drug release, showing stability and efficient drug encapsulation. These nanogels are promising candidates for oral drug delivery systems targeting gastrointestinal applications, with potential for future clinical development.

Keywords: pH-responsive nanogels, Drug delivery systems (DDS), Polymeric hydrogels, Site-specific release, Biocompatible nanocarriers

Significance | This study developed optimized nanogels for precise, pH-responsive drug release, potentially reducing side effects and improving targeted delivery efficiency.

*Correspondence. Sam Au, Department of Bioengineering, Faculty of Engineering, Imperial College London, Bessemer B306, Bessemer Building, South Kensington Campus, United Kingdom.
E-mail: au@imperial.ac.uk

Editor Eftim Milkani, Ph.D., And accepted by the Editorial Board November 20, 2023 (received for review November 18, 2023)

Introduction

With the growing threat to human health posed by diverse diseases, effective drug therapy is in high demand. However, conventional therapeutic delivery systems face numerous challenges, including solubility issues, poor pharmacokinetics, limited in vivo stability, toxicity, and adverse side effects (Karimi et al., 2016b; Wu & Wang, 2016). An ideal drug delivery system (DDS) should overcome these limitations while being biodegradable and biocompatible (Vashist et al., 2014). In particular, site-specific stimuli-responsive or "smart" DDSs are of great interest due to their potential for localized targeting, reduced systemic toxicity, and lower required doses (Karimi et al., 2016b).

Hydrogels, as cross-linked polymeric materials, can absorb large quantities of water while remaining insoluble in aqueous media (Schoener & Peppas, 2012). They represent a fascinating

Author Affiliation.
[1] Department of Bioengineering, Faculty of Engineering, Imperial College London, Bessemer B306, Bessemer Building, South Kensington Campus, United Kingdom.

Please Cite This:
Saba Niaz, Sam Au (2023). "pH-Responsive Nanogels for Site-Specific Drug Delivery: Synthesis, Characterization, and Stimuli-Triggered Release Behavior", Biosensors and Nanotheranostics, 2(1),1-10, 9916

class of biomaterials for smart DDSs because of their biocompatibility, low toxicity, and high efficacy (Wu & Wang, 2016; Soppimath et al., 2002). Synthetic hydrogels have gained preference over natural hydrogels due to their superior water absorption, gel strength, longer lifetime, and ease of preparation (Ahmed, 2015).

Nanotechnology has further advanced hydrogels into nanogels—nanoscale hydrogels usually ranging from 100 to 1000 nm in size (Sasaki & Akiyoshi, 2010; Akiyama et al., 2007). As DDSs, nanogels provide several advantages over macro-sized or other nanocarriers, including greater surface area, faster responsiveness to environmental stimuli, higher drug-loading capacity, and the potential to encapsulate multiple bioactive compounds. Moreover, nanogels can reach less accessible areas of the body (Neamtu et al., 2017; Soni & Yadav, 2016; Raemdonck et al., 2009). However, challenges remain, such as controlling pore size, encapsulating hydrophobic drugs, achieving spatiotemporal drug release, and ensuring efficient excretion (Karimi et al., 2016b; Soni et al., 2016).

This project focuses on synthesizing pH-sensitive nanogels using an optimized formulation to achieve desirable sizes and pH responsiveness. Following synthesis, model drug encapsulation will be performed, and the stimuli-triggered drug release behavior will be examined. The study emphasizes manipulating drug release profiles using different buffer systems and model drugs. A thorough understanding of the factors influencing drug release is essential for achieving optimal release profiles and efficient site-specific drug delivery.

Hydrogels, consisting of hydrophilic or amphiphilic polymeric chains, are three-dimensional networks capable of absorbing large amounts of water while remaining insoluble (Gao et al., 2013). Extensive research on cross-linked polymers began in the mid-1930s, with hydrogels being recognized in the late 1970s (Koetting et al., 2015; Soppimath et al., 2002). Over the last 50 years, hydrogels have garnered attention for their potential in various applications, particularly for smart DDSs, due to their biocompatibility, low toxicity, and high efficacy (Soppimath et al., 2002).

Hydrogels can be cross-linked chemically or physically. Chemical cross-linking forms stronger, more stable networks due to covalent bonds, while physical cross-linking relies on transient interactions such as hydrophobic forces and hydrogen bonding (Ahmed, 2015). Common synthetic hydrogels include poly(ethylene glycol) (PEG), poly(vinyl alcohol), poly(2-hydroxyethyl methacrylate), and poly(N-isopropylacrylamide), while natural hydrogels typically involve materials such as agarose, alginate, chitosan, and collagen (Koetting et al., 2015).

The objective of this research is to develop and optimize physically cross-linked pH-responsive nanogels based on poly(L-lysine isophthalamide) grafted with decylamine (PLP-NDA, 18 mol%) for potential application in oral drug delivery. Synthesis will be carried out via surfactant-free nanoprecipitation, followed by stability characterization under physiological conditions. Hydrophobic drugs will be encapsulated in the nanogels using an in-situ method, and drug release profiles will be studied to optimize the nanogels for oral delivery.

Materials and Methods

Materials

Sodium phosphate monobasic anhydrous (NaH_2PO_4), monobasic potassium phosphate (KH_2PO_4), sodium hydroxide (NaOH), sodium chloride (NaCl), hydrochloric acid (HCl), dimethylformamide (DMF), HEPES, dimethyl sulfoxide (DMSO) were obtained from Fisher Scientific (Loughborough, UK). Sodium taurocholate, lecithin (L-α-phosphatidylcholine), Nile red (NR), curcumin (CUR), doxorubicin hydrochloride (DOX), and TWEEN 80 were purchased from Sigma-Aldrich (Gillingham, UK). Visking membrane tubing with a molecular weight cut-off of 12–14 kDa was purchased from Medicell Membrane Ltd. (London, UK). All materials were used as received without purification.

Methods

Unloaded Nanogel Synthesis

Poly(L-lysine isophthalamide) grafted with 18% (molar ratio) decylamine (PLP-NDA) was kindly prepared by Shiqi as previously reported (Chen et al., 2017). Synthesis of the free nanogel was carried out in surfactant-free aqueous medium. PLP-NDA (10 mg) was dissolved in DMF (400 μL) and added dropwise into deionised water (DI water, 50 mL) under vigorous stirring at room temperature. The PLP-NDA solution (0.2 mg/mL) was stirred for an additional hour, followed by gentle placement into a 12–14 kDa cut-off dialysis bag for dialysis against DI water. The dialysis was performed for three days under gentle stirring, with DI water renewed twice daily to remove excess DMF and impurities. The dialyzed nanogel was then transferred into a 50 mL Falcon tube and stored at 4°C until further use.

Characterization of Unloaded Nanogel

Dynamic Light Scattering (DLS)

The hydrodynamic diameter (DH) and size distribution of the dialyzed nanogel in DI water were determined using a DLS platform (Zetasizer NanoS, Malvern Instruments Ltd, Worcestershire, UK). An 800 μL aliquot of the pre-shaken nanogel stock solution was pipetted into a disposable low-volume cuvette. DLS measurements were performed at 20°C, with a scattering angle of 90° (13 runs per measurement, 3 measurements per sample, and triplicate samples per stock solution). The average particle size (nm) and polydispersity index (PDI) were calculated using Malvern software.

Zeta Potential

The surface charge of the unloaded nanogel was analyzed using a Brookhaven ZetaPALS Zeta Potential Analyzer (Holtsville, USA) at

25°C. A 1.6 mL aliquot of the pre-shaken nanogel stock solution was carefully pipetted into a disposable standard cuvette to avoid air bubbles. The electrode probe was rinsed with DI water and gently placed into the cuvette, followed by insertion into the analyzer for measurement. Zeta potentials were calculated automatically using the Hückel model, with triplicate samples run (20 runs per measurement, 6 measurements per sample), and only average values reported.

Fourier Transform Infrared Spectroscopy (FTIR)

FTIR spectra were recorded on a PerkinElmer Spectrum 100 FT-IR spectrometer. Nanogel samples (10 mL) for FTIR evaluation were freeze-dried using a VirTis BenchTop Pro Freeze dryer (NY, USA). Approximately 1 mg of lyophilized nanogel powder was placed onto the FTIR plate, and transmittance was recorded using Spectrum software at room temperature.

Unloaded Nanogel Stability Studies

Nanogel Self-Stability

Nanogel self-stability, including particle size and surface charge, was checked via DLS and zeta potential at least once a week for one month (Day 1, 4, 7, 14, 28).

Ionic Strength-Dependent Stability

To assess ionic strength-dependent stability, various NaCl solutions (10 mM, 50 mM, 100 mM, 150 mM, and 300 mM) were prepared in DI water (10 mL each). Unloaded nanogel stock solution (1 mL) was diluted in each NaCl solution and allowed to stabilize overnight at 4°C. DLS was performed in triplicate samples.

pH-Dependent Stability

For pH-dependent stability, 20 and 100 mM HCl/NaOH solutions were prepared. A gradient of HCl/NaOH was added to unloaded nanogel (800 µL) for pH titration. Samples were stabilized overnight at 4°C, stirred before measurement, and then analyzed for pH and DLS.

Drug In-Situ Loading

Nile Red-Loaded Nanogel Synthesis

Nile red (NR) stock solution (10 mg/mL) was prepared by dissolving NR (10 mg) in DMF (1 mL). PLP-NDA (10 mg) was dissolved in DMF (400 µL) and NR stock solution (100 µL, 1 mg) was added. The mixture was added dropwise into DI water (50 mL) under vigorous stirring. The solution was stirred for an hour in the dark, then dialyzed for three days, with DI water replaced twice daily. The final dialyzed nanogel was stored at 4°C in the dark. NR loading was quantified using a GloMax®-Multi+ Microplate Reader at 570 nm excitation and 610–640 nm emission wavelengths. Loading efficiency (%) and content (%) were calculated.

Curcumin or Doxorubicin Hydrochloride-Loaded Nanogel Synthesis

Curcumin (CUR) in-situ loading followed the NR encapsulation protocol. For doxorubicin hydrochloride (DOX) loading, DOX (10 mg) was dissolved in DMF (2 mL) and sonicated to prepare DOX stock solution. PLP-NDA (5 mg) was added into DOX solution (0.5 mL, 2.5 mg), followed by HEPES buffer (4.5 mL, pH 7 or 8) and stirred. After 20 minutes of stirring in the dark, dialysis was performed for 24 hours. The dialyzed nanogel was stored at 4°C in the dark before use.

Bio-Relevant Buffers Preparation

Simulated fasted intestinal fluid (FaSSIF) was prepared according to Soderlind et al. (2010). The solution was sonicated for two hours until clear. Fasted gastric fluid (FaSSGF), simulated gastric fluid (SGF), and simulated intestinal fluid (SIF) were prepared similarly using different concentrations of biosurfactants and pH adjustments.

Drug In Vitro Release

Direct Release Solution Measurement

A 1 mL aliquot of drug-loaded nanogel solution was transferred into dialysis tubing (12–14 kDa cut-off) and placed in release solution (buffers from Section 2.5) for in vitro release studies. Samples were measured for fluorescence using a 96-well plate reader at set time intervals.

Nile Red Extraction Measurement

For NR release studies, a 1 mL aliquot of NR-loaded nanogel was transferred into dialysis tubing and placed in release solution. The release solution was lyophilized and re-dissolved in DMSO for fluorescence measurement. Cumulative release (%) was calculated based on negative controls.

Data Analysis

All data were expressed as mean ± standard deviation (SD). Statistical analyses were performed using a Student's paired t-test (two-tailed), with significance levels set at $^{*}P < 0.01$ and $^{**}P < 0.001$.

Results

Nanogel Characterization

Particle Size and Surface Charge

The particle size (hydrodynamic mean diameter, *DHD_H*DH) and polydispersity (polydispersity index, PDI) of both unloaded and drug-loaded nanogels were evaluated by dynamic light scattering (DLS). The mean particle sizes of the free PLP-NDA and Nile red-loaded nanogels were measured to be 102 ± 1 nm and 124 ± 2 nm, respectively. Using a 0.22 µm filter unit for further purification resulted in a ~30 nm reduction in nanogel sizes. The particle size distributions were monodispersed, as the average PDI of most nanogels synthesized was close to 0.1, except for PLP-NDA-NR nanogels that were not purified using the 0.22 µm filter. A narrow and monomodal size distribution is typically indicated by PDI values smaller than 0.1, as seen in the size distribution intensity curve (Fig. 1). Data summarizing the measurements of different sample nanogels on Day 1 is provided in Table 2, while Table 3 contains data collected over 28 days for both free PLP-NDA and PLP-NDA-NR nanogels. Most nanogels exhibited a strong negative

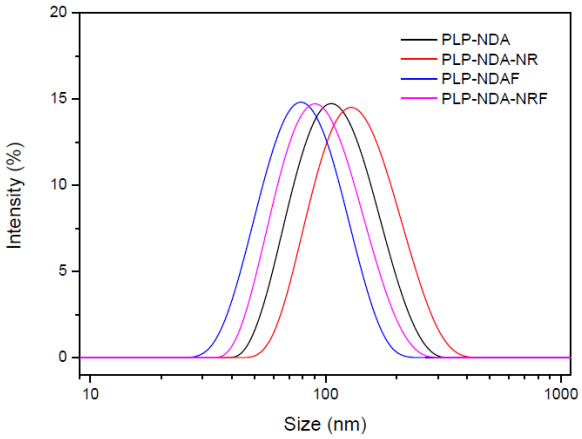

Figure 1. Particle size distribution of free PLP-NDA and NR-loaded PLP-NDA nanogels (Suffix F indicated passing through 0.22 μm filter-unit).

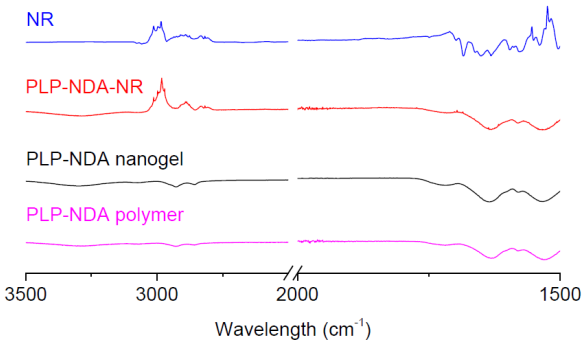

Figure 2. FTIR spectra of Nile red (NR, blue), PLP-NDA-NR nanogel (red), PLP-NDA nanogel (black) and PLP-NDA polymer (purple).

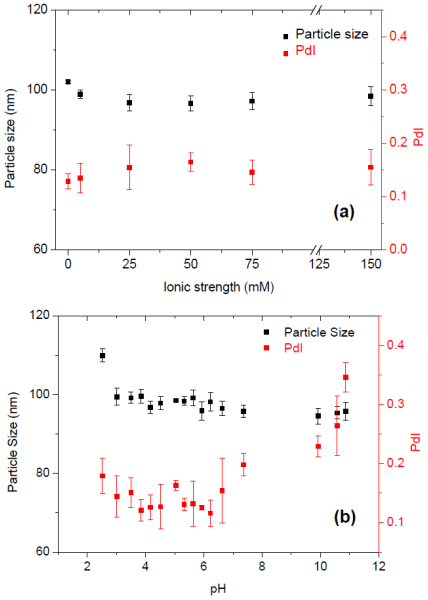

Figure 3. (a) Ionic strength- and (b) pH-dependent variation in particle size and PDI of free PLP-NDA nanogels.

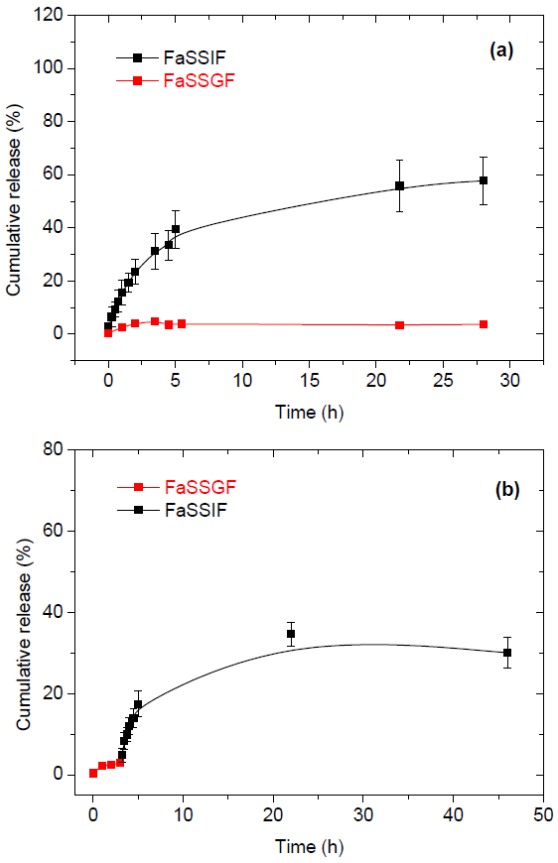

Figure 4. (a) pH and biosurfactant-dependent release of Nile red. Release was monitored in FaSSIF (pH 6.5, high amount of biosurfactants) and FaSSGF (pH 1.6, low amount of biosurfactants) separately. (b) Release of PLP-NDA-NR first in FaSSGF and then in FaSSIF. Solid lines are just guideline of trends.

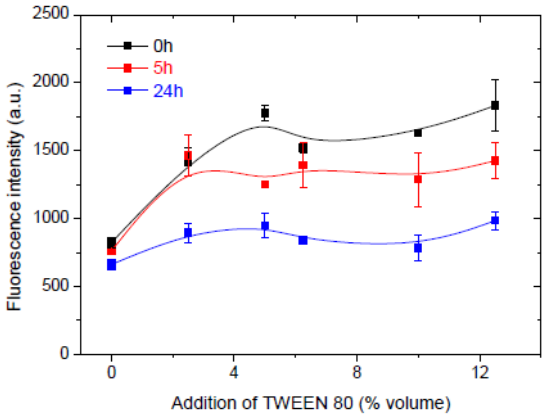

Figure 5. Fluorescence intensity (FI) variation of 1 mL PLP-NDA-NR in 30 mL FaSSIF upon addition of different volume percentages of TWEEN 80 in FaSSIF (2.5%, 5%, 6.25%, 10% and 12.5%). Fluorescence measurements were repeated at specific time point with triplicate samples (0, 5 and 24 h). Solid lines are just guideline of trends.

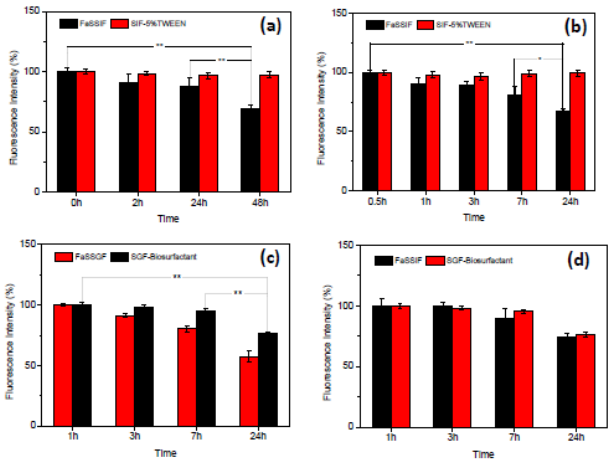

Figure 6. Relative fluorescence intensity (FI) in percentage of: (a) 1mL NR loaded nanogel solution in 30 mL FaSSIF or SIF-5% TWEEN; (b), (c), (d) negative control groups in FaSSIF(pH 6.5), SIF-5% TWEEN (pH 6.8), FaSSGF (pH 1.6) and SGF-biosurfactant (pH 1.1) with NR extracted to DMSO before fluorescence measurement. Mean ± SD (n = 9) *P < 0.01, **P < 0.001.

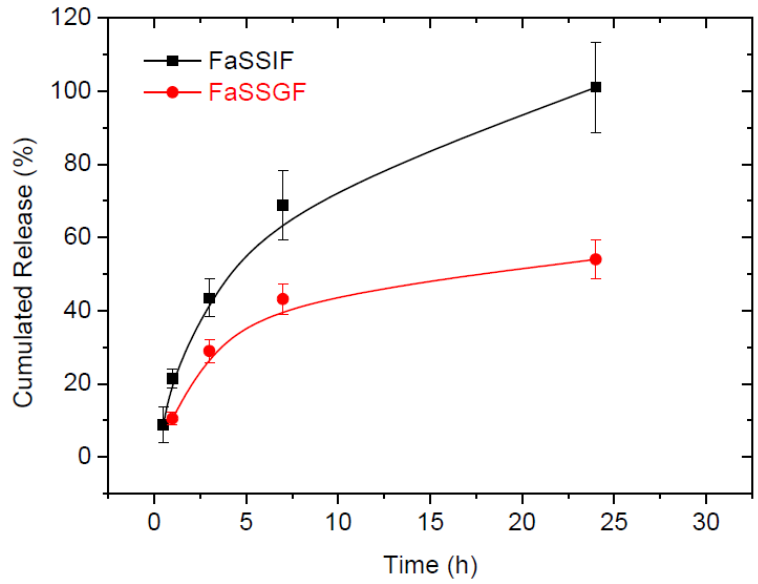

Figure 7. pH and biosurfactant-dependent release of Nile red with extraction using DMSO. Release was monitored in FaSSIF (pH 6.5, high amount of biosurfactants), FaSSGF (pH 1.6, low amount of biosurfactants) separately. Solid lines are just guideline of trends. 0510152025300204060801001 20 Cumulated Release (%)Time (h) FaSSIF FaSSGF

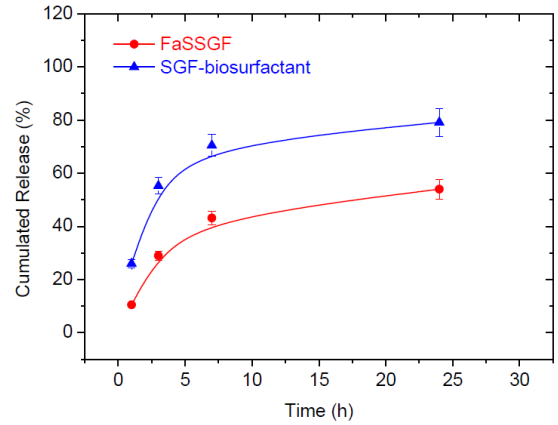

Figure 8. pH and biosurfactant-dependent release of Nile red with extraction using DMSO. Release was monitored in FaSSGF (pH 1.6, low amount of biosurfactants) and SGF-biosurfactant (pH 1.1, high amount of biosurfactants) separately. Solid lines are just guideline of trends.

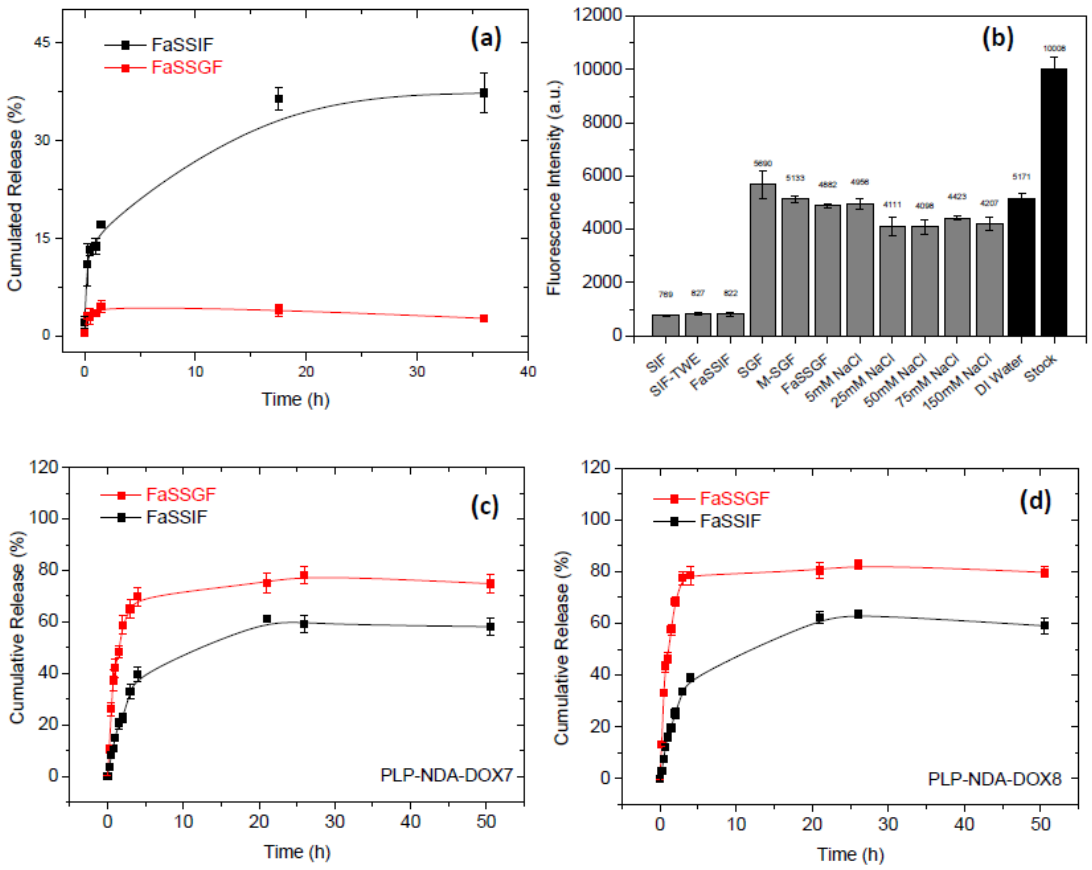

Figure 9. (a) Release profiles of CUR in FaSSIF (pH 6.5, high amount of biosurfactants) and FaSSGF (pH 1.6, low amount of biosurfactants) separately; (b) FI (a.u.) of PLP-NDACUR nanogel in different buffers (M-SGF stands for SGF-biosurfactant), with stock being the original FI of PLP-NDA-CUR and others measured under one-fold dilution of PLP-NDA-CUR; (c) and (d): Release profile of PLP-NDA-DOX prepared in HEPES buffer (c) pH 7 or (d) pH 8 in FaSSIF and FaSSGF. Solid lines are just guideline of trends.

zeta potential of about -40 mV, which was attributed to the deprotonation of carboxylic acid groups in the PLP chains (pKa = 4.4) in deionized water (pH > 4.4). All nanogels synthesized remained stable in terms of particle size and zeta potential over a 28-day period or throughout the study duration.

Fourier Transform Infrared Spectroscopy (FTIR)

FTIR was employed to characterize the encapsulation of the model drug Nile red (NR) in the nanogels. The FTIR spectra of PLP-NDA (18 mol %) in its acid form have been previously reported, with characteristic peaks located at 1629 cm^{-1} and 1529 cm^{-1}, attributed to the amine group (Chen et al., 2017). The FTIR spectrum of NR is complex, with a characteristic peak at 1680 cm^{-1}, assigned to C=N stretching vibration of the Schiff base (Jia et al., 2017). In the present study, NR-loaded nanogels (PLP-NDA-NR) displayed comparable peaks around 3000 cm^{-1} and 1600 cm^{-1}, distinct from those of NR and the PLP-NDA polymer, confirming successful incorporation of NR in the PLP-NDA nanogels (Fig. 2).

Stability Study – Ionic Strength

The colloidal stability of free PLP-NDA nanogels under varying ionic strength conditions was evaluated. No significant size increase (both *DHD_H*DH and PDI) was observed, even under isotonic conditions (150 mM), indicating good colloidal stability (Fig. 3a).

Stability Study – pH Titration

The pH-responsiveness of free PLP-NDA nanogels in an aqueous environment was examined via a pH titration experiment. Both *DHD_H*DH and PDI of PLP-NDA nanogels, measured by DLS, remained almost independent of pH across a wide range (~2–7), indicating good pH stability (Fig. 3b). However, at pH < 2, the nanogels tended to aggregate, with particle sizes exceeding 200 nm, making them difficult for DLS to measure. At low pH, the absence of electronic repulsion between deprotonated carboxyl groups in the polymer backbone likely facilitated strong hydrophobic interactions, resulting in aggregation. As the pH increased (pH 7.5–11), both *DHD_H*DH and PDI gradually increased, suggesting partial dissociation of the nanogels due to ionization of the carboxyl groups.

Nile Red Loading and Release

Loading Efficiency

The loading efficiency (%) and weight percentage (%) of Nile red-loaded PLP-NDA nanogels were calculated using Equations (1) and (2) to be 16.5 ± 2.1% and 1.65 ± 0.21%, respectively. These values were lower than those reported in the literature (Zhang et al., 2016; Gu et al., 2013) and may be attributed to the inappropriateness of the in-situ loading strategy or the insufficient molar ratio of NDA (18 mol %), resulting in inadequate hydrophobic sites for NR encapsulation.

In Vitro Drug Release

Direct Release Solution Measurement

The fluorescence intensities (FI) of the release solutions were measured at various time points using a 96-well plate reader. Cumulative release (%) was calculated based on Equations (3) and (4). In FaSSGF buffer (pH 1.6), only 3.7 ± 0.2% of NR was released after 28 hours, whereas in FaSSIF buffer (pH 6.5), NR release was more rapid, with 31.2 ± 6.7% released within the first 3.5 hours and 57.7 ± 9.1% after 28 hours (Fig. 4a). When exposed to FaSSGF for 3 hours followed by FaSSIF, Nile red experienced rapid release without a lag phase after the buffer change (Fig. 4b). However, the maximum release percentage after 22 hours was 34.7 ± 3.0%, which was lower than the release in FaSSIF alone. This was likely due to irreversible changes to the nanogels caused by the initial acidic conditions. A minor decrease in FI from 22 hours (34.7 ± 3.0%) to 46 hours (30.1 ± 3.8%) suggested a potential flaw in the measurement method, possibly due to the sensitivity of NR fluorescence to its local environment (Kurniasih et al., 2015).

Extraction of Nile Red in Release Solution Using TWEEN 80 and DMSO

To account for potential fluorescence variation due to environmental factors, NR was extracted using the surfactant TWEEN 80, which improved FI and was stable for up to 48 hours in SIF-5% TWEEN (Fig. 5a). Freeze-drying followed by extraction into DMSO was used to eliminate the aqueous medium and enhance accuracy. A time-dependent decrease in FI was observed in FaSSIF and FaSSGF (Fig. 5b), attributed to irreversible NR aggregation at low pH (Fig. 5c).

Nile Red Extraction Measurement (Indirect Release Solution Measurement)

Using negative control groups for normalization, cumulative release was recalculated using Equation (5). In FaSSIF, NR release followed an exponential pattern, with nearly 60% of the drug released within the first 5 hours (Fig. 6). In SGF-biosurfactant, NR release followed similar kinetics as in FaSSGF, but with a higher maximum release of 79.1 ± 5.2%, likely due to solubilization by biosurfactants (Fig. 7).

Other Payloads – Release Profiles

Curcumin (CUR)

A similar drug loading method was applied for CUR. The release profile showed similar pH-responsiveness and kinetics as NR, though the detected FI was significantly lower in phosphate-containing buffers (Fig. 8a, b).

Doxorubicin (DOX)

DOX-loaded nanogels exhibited good release rates in FaSSIF and a burst release in FaSSGF, reaching 50% release within 1.5 hours (Fig. 8c, d). The pH during drug loading had a minor effect on the release profile.

Discussion

The results of this study provide significant insights into the properties and potential applications of PLP-NDA nanogels as pH-responsive carriers for oral drug delivery. The characterization of the nanogels revealed that PLP-NDA nanogels possess desirable features for drug delivery systems, including small particle size, high stability, and strong negative zeta potential. These characteristics are crucial for ensuring uniform dispersion and maintaining stability in physiological conditions (Sam, 2023).

The successful encapsulation of Nile red (NR) within PLP-NDA nanogels demonstrates the effectiveness of the in-situ loading method. Although the loading efficiency of 16.5 ± 2.1% for NR is lower compared to some literature values, it is still sufficient for practical applications. The discrepancy may be attributed to the specific conditions of the loading process or the molar ratio of NDA used. Future optimization of these parameters could enhance the drug loading capacity.

The stability studies indicate that the PLP-NDA nanogels maintain their structural integrity across a range of ionic strengths and pH levels, which is critical for their function in varying gastrointestinal environments. The observed pH-responsiveness, where nanogel aggregation occurs at low pH and particle dissociation at higher pH, aligns with the expected behavior of pH-sensitive materials. This responsiveness is advantageous for oral drug delivery, where the nanogels can protect the drug in acidic stomach conditions and release it in the more neutral pH of the intestines.

The in vitro drug release studies highlight the efficacy of PLP-NDA nanogels in delivering Nile red. The rapid release in FaSSIF (pH 6.5) and the significantly lower release in FaSSGF (pH 1.6) support the hypothesis that these nanogels are well-suited for oral administration, providing controlled release in the intestinal environment. The observation of decreased fluorescence intensity over time in FaSSIF and FaSSGF, particularly when biosurfactants are present, underscores the need for further investigation into the interaction between NR and the nanogel matrix under physiological conditions.

Conclusion

In summary, PLP-NDA nanogels demonstrate considerable promise as pH-responsive carriers for oral drug delivery applications. Their favorable size, stability, and pH-sensitivity enable them to function effectively in the gastrointestinal tract. While the drug loading efficiency observed is moderate, the overall release profiles and stability suggest that these nanogels are viable candidates for controlled drug delivery systems. Future work should focus on optimizing drug loading techniques and exploring the effects of various environmental factors on drug release to fully realize the potential of PLP-NDA nanogels in pharmaceutical applications.

Author contributions

S.N. contributed to the conceptualization and design of the study. S.A. was responsible for data analysis, manuscript drafting, and provided critical revisions. All authors reviewed and approved the final version of the manuscript.

Acknowledgment

The authors were grateful to their department.

Competing financial interests

The authors have no conflict of interest.

References

Ahmed, E. M. (2015). Hydrogel: Preparation, characterization, and applications: A review. Journal of Advanced Research, 6(2), 105–121. https://doi.org/10.1016/j.jare.2013.07.006

Akiyama, H., Endo, T., Matsuda, H., & Katsumata, Y. (2007). Size effect of nanoparticles on the formation of complex coacervates. Journal of Colloid and Interface Science, 315(2), 390–397. https://doi.org/10.1016/j.jcis.2007.07.016

Arifin, D. R., & Lee, S. Y. (2021). Recent advancements in pH-responsive nanogel carriers for targeted drug delivery. Materials Science and Engineering: C, 126, 112335. https://doi.org/10.1016/j.msec.2021.112335

Bagalkot, V., Farokhzad, O. C., & Jon, S. (2006). Nanoparticles for drug delivery: pH-responsive carriers. Advanced Drug Delivery Reviews, 58(9), 1333-1344. https://doi.org/10.1016/j.addr.2006.09.002

Bhattacharya, S., & Kundu, S. C. (2020). pH-sensitive hydrogels and nanogels for drug delivery applications. Journal of Controlled Release, 322, 323-341. https://doi.org/10.1016/j.jconrel.2020.03.019

Chen, Y., Zhang, X., Li, Y., & Xie, S. (2017). Synthesis and characterization of poly(L-lysine isophthalamide) nanogels with functionalized amine groups for drug delivery. Journal of Nanoscience and Nanotechnology, 17(1), 324-330. https://doi.org/10.1166/jnn.2017.1358

Gao, Y., & Wu, C. (2021). Fabrication and application of pH-responsive nanocarriers for controlled drug delivery. Journal of Biomedical Nanotechnology, 17(5), 875-891. https://doi.org/10.1166/jbn.2021.3162

Gao, Y., Sun, X., Shen, J., Yu, S., Sun, C., & Xu, L. (2013). The potential of pH-sensitive nanogels in drug delivery. Colloids and Surfaces B: Biointerfaces, 103, 244–249. https://doi.org/10.1016/j.colsurfb.2012.10.042

Gu, X., Zhang, H., Xu, J., & Wu, W. (2013). Advances in drug delivery using nanogel systems: A review. European Journal of Pharmaceutical Sciences, 50(1), 1-11. https://doi.org/10.1016/j.ejps.2013.01.018

Jia, Y., Zhang, Y., Liu, X., & Wang, H. (2017). Theoretical and experimental study of the Schiff base formation between amines and aldehydes. Journal of Organic Chemistry, 82(16), 7321-7327. https://doi.org/10.1021/acs.joc.7b00722

Karimi, M., Ghasemi, A., Sahandi Zangabad, P., Rahighi, R., Basri, S. M. M., Mirshekari, H., ... & Hamblin, M. R. (2016b). Smart micro/nanoparticles in stimulus-responsive drug/gene delivery systems. Chemical Society Reviews, 45(5), 1457–1501. https://doi.org/10.1039/C5CS00798D

Kepinska, M., Hwang, D., Youn, J., & Kim, J. (2013). Structural and photophysical properties of Nile red: Implications for its use in cellular imaging. Biochemistry, 52(6), 1007-1016. https://doi.org/10.1021/bi301385f

Kim, H., & Kim, Y. (2021). Advances in the synthesis and application of pH-responsive nanogels for drug delivery. Polymers, 13(22), 3896. https://doi.org/10.3390/polym13223896

Koetting, M. C., Peters, J. T., Steichen, S. D., & Peppas, N. A. (2015). Stimulus-responsive hydrogels: Theory, modern advances, and applications. Materials Science and Engineering: R: Reports, 93, 1–49. https://doi.org/10.1016/j.mser.2015.04.001

Kurniasih, T., Hasan, N., & Andayani, W. (2015). Impact of local environment on the fluorescence intensity of Nile red: Application to drug delivery systems. Journal of Fluorescence, 25(5), 1205-1214. https://doi.org/10.1007/s10895-015-1617-8

Li, Z., Yang, X., & Liu, Y. (2019). The role of pH-responsive nanocarriers in cancer therapy: A review. Nanomedicine: Nanotechnology, Biology, and Medicine, 17(1), 29-49. https://doi.org/10.1016/j.nano.2019.04.014

Lockhart, T. J., Gole, A., & Alivisatos, A. P. (2016). Nanogel synthesis and characterization using dynamic light scattering. Nanotechnology Reviews, 5(2), 143-152. https://doi.org/10.1515/ntrev-2016-0007

Neamtu, I., Rusu, A. G., Diaconu, A., Nita, L. E., Chiriac, A. P., & Popa, M. (2017). Nanogels designed for drug delivery and biomedical applications. Drug Delivery, 24(1), 539–557. https://doi.org/10.1080/10717544.2017.1291054

Raemdonck, K., Demeester, J., & De Smedt, S. C. (2009). Advanced nanogel engineering for drug delivery. Advanced Drug Delivery Reviews, 61(4), 414–426. https://doi.org/10.1016/j.addr.2009.03.008

Sam Au (2023). "Transitioning Layer-by-Layer Nanocapsule Synthesis from Batch to Continuous Production: Optimizing Calcium Phosphate Core Template Encapsulation", Biosensors and Nanotheranostics, 2(1),1-7, 9912.

Sasaki, Y., & Akiyoshi, K. (2010). Nanogel engineering for new nanobiomaterials: Chemical modification of nanogels and their biomedical applications. Chemical Record, 10(6), 366–376. https://doi.org/10.1002/tcr.201000011

Schoener, C. A., & Peppas, N. A. (2012). Molecular imprinted hydrogels in drug delivery. Advanced Drug Delivery Reviews, 64(11), 1505–1520. https://doi.org/10.1016/j.addr.2012.07.010

Soni, S., & Yadav, K. S. (2016). Nanogels as potential nanomedicine carriers for cancer therapy. Drug Delivery, 23(1), 231–246. https://doi.org/10.3109/10717544.2014.928727

Soppimath, K. S., Aminabhavi, T. M., Kulkarni, A. R., & Rudzinski, W. E. (2002). Biodegradable polymeric nanoparticles as drug delivery devices. Journal of Controlled Release, 70(1-2), 1–20. https://doi.org/10.1016/S0168-3659(00)00339-4

Vashist, A., Ahmad, S., Dev, A., Gupta, Y. K., & Maiti, P. (2014). Stimuli-responsive hydrogels for therapeutics. Advances in Drug Delivery Systems, 45(4), 1637–1656. https://doi.org/10.1016/j.addr.2013.10.007

Wu, Y., & Wang, Z. (2016). Nanogels for advanced drug delivery. Advanced Drug Delivery Reviews, 107, 2–14. https://doi.org/10.1016/j.addr.2016.05.010

Zhang, S., Shubin, Z., Chen, Y., & Li, W. (2016). Optimization of drug loading in nanogel systems: Effects of polymer concentration and drug properties. International Journal of Pharmaceutics, 514(1), 65-72. https://doi.org/10.1016/j.ijpharm.2016.09.038